Research Article

Cryogenic features and stages in Late Quaternary subaerial sediments of the Lower Volga region

N.A. Taratunina[a,b]* 🆔, R.N. Kurbanov[a,c], V.V. Rogov[a], I.D. Streletskaya[a], T.A. Yanina[a], D.A. Solodovnikov[d] and T. Stevens[e] 🆔

[a]Faculty of Geography, Lomonosov Moscow State University, Moscow, Russia; [b]Institute of Archaeology and Ethnography, Siberian Branch RAS, Novosibirsk, Russia; [c]Institute of Geography RAS, Moscow, Russia; [d]Volgograd State University, Volgograd, Russia and [e]Department of Earth Sciences, Uppsala University, Uppsala, Sweden

Abstract

Situated at the southernmost limits of the late Pleistocene Eurasian permafrost zone, the loess–paleosol sequences of the Lower Volga region contain numerous traces of cryogenesis. Cryogenic features are represented by thin vertical wedges in loess and paleosols, and involutions and wedges in alluvial deposits. Here we describe and interpret four stages of cryogenesis during the late Pleistocene, based on analysis of cryogenic structure morphology, morphoscopy of quartz grains, and micromorphology of subaerial sediments, in addition to calculation of the Cryogenic Weathering Index and a new luminescence chronology derived from published ages. These stages differ in type and distribution of cryostructures and formed in different paleogeographic conditions. Stage I, dated 95–90 ka (Marine Isotope Stage [MIS] 5b), is characterized by the existence of continuous permafrost in northern part of the Lower Volga valley. Stage II (75–70 ka, MIS 5a/MIS 4) is characterized by dry and cold conditions and widespread permafrost. During stage III (52–45 ka, MIS 3b/c), the permafrost was thin and of sporadic distribution. Stage IV (37–35 ka, MIS 3a) is characterized by thin and rare sporadic permafrost. The processes of cryogenic transformation of sediments in the region during these stages took place under both permafrost and seasonal frost conditions. The results obtained significantly improve current understanding of the extent of the permafrost in the south of the East European Plain during the late Pleistocene.

Keywords: Loess, Paleo-permafrost, Cryogenic Weathering Index, Luminescence dating, East European Plain, Caspian Sea, Climate change

(Received 31 May 2023; accepted 17 January 2024)

Introduction

Periglacial permafrost was a widespread phenomenon on the East European Plain (EEP) during the late Pleistocene, with considerable evidence of the existence of past permafrost in the form of various cryogenic structures in cold stage sediments (Velichko, 1973, 2002; Velichko et al., 1996; Sycheva, 2012; Streletskaya, 2017). These structures form cryogenic horizons that are important chronostratigraphic markers. However, at present, there is no detailed reconstruction of cryogenic stages on the EEP and the conditions under which these cryogenic processes developed and there is no clear agreement on the maximum extent of the permafrost area during the late Pleistocene. As the processes occurring in permafrost control relief and sedimentation and largely determine the physical and chemical changes in sediments in permafrost areas, it is critical to address this gap. Furthermore, cryogenic horizons are of great stratigraphic importance, because they can serve as a benchmark for the development of regional stratigraphic schemes and significantly refine

paleogeomorphological reconstructions. In addition to the stratigraphic context, a detailed study of the structure of cryogenic forms, use of the paleo-analogs method, and comparisons to modern permafrost in loess (e.g., Rasmussen et al., 2023) allow reconstruction of the conditions during the formation of cryogenic forms and clarification of existing paleogeographic reconstructions.

There are some features in loess deposits that are considered characteristic for sediments from permafrost areas: (1) a predominance of a coarse silt fraction in loess sediments is interpreted as an indicator of cold and dry conditions (Deng et al., 2010); (2) a prevalence of coarse silt aggregates (which form from fine silt or clay particles) is associated with the processes occurring during cyclic freezing and thawing (Zhai et al., 2021); (3) quartz particles from different sedimentation environments are supplemented by numerous angular grains with chips and sharp edges, which indicate a cryogenic mechanism in their destruction (Woronko and Pisarska-Jamrozy, 2015; Kalinska-Nartiša et al., 2017; Költringer et al., 2021a); and (4) high porosity that can be caused by the formation of ice crystals during the freezing of deposits (see Rasmussen et al. [2023] for an example of current permafrost loess with varying ice contents).

Furthermore, in the southeastern part of the EEP, terrestrial sediments interact with marine sedimentary phases associated

with transgressions of the Caspian Sea (Költringer et al., 2021b). The transgression–regression history of the Caspian Sea and the waterbody's water balance over the Pleistocene remain poorly constrained (Gelfan and Kalugin, 2021; Panin et al., 2021), and the causes of major paleogeographic events that determined sea-level changes are not completely clear. The source of water for the largest Late Quaternary sea-level rise—the Khvalynian transgression, when sea-level reached +48 m amsl (above mean global sea level) in a relatively short time (Kurbanov et al., 2021, 2023)—is a topic of debate (Koriche et al., 2022). Indeed, cryogenesis in the region's deposits may be one of the possible factors that led to sea-level changes. If permafrost sediments had high ice content, then rapid thawing of permafrost combined with increased flow of the Volga River fed by permafrost thawing and ice melting would increase discharge into the Caspian basin, and raise sea level (Gelfan and Kalugin, 2021). As such, reconstruction of the type and mechanisms of and conditions for the formation of ancient permafrost in the Lower Volga region (LVR) will be a step toward a better understanding of the water balance of the Caspian Sea in the late Pleistocene. Here we address this knowledge gap using cryofeatures preserved in late Pleistocene loess of the LVR, in the north Caspian Lowland, an area lying at the limit of proposed Pleistocene permafrost distribution.

Study Area

The Caspian Lowland lies at the limit of possible late Pleistocene (continuous?) permafrost, and the distribution of permafrost in the region itself is debated (Velichko, 2002). Over a significant extent of the Volga-Akhtuba valley (LVR), a series of sedimentary sections are exposed that contain a unique record of the Quaternary history of sea-level fluctuations and climate evolution in the Caspian Sea (Költringer et al., 2021b; Kurbanov et al., 2021). However, most previous publications contain only short and fragmentary descriptions of the paleogeographic conditions of the regressive epochs of the Caspian Sea, which can be reconstructed on the basis of the study of subaerial deposits, mainly the loess–paleosol sequences, and few have concentrated on detailed analysis of cryofeatures in the deposits (Moskvitin, 1962).

The insufficiency of data on the reconstruction of landscapes and climate during the long-term Caspian Sea Atelian regression (Marine Isotope Stage [MIS] 4 to the first half of MIS 3) is a function of: (1) the small number of sections studied by modern methods and (2) the primary focus of past work being directed toward descriptions of the marine sediments of various transgressive stages of the Caspian Sea in the region (Svitoch, 2014). However, a reconstruction of the evolution of permafrost processes during the late Pleistocene based on a study of subaerial deposits and analysis of their influence on the various sedimentation features may allow a better understanding of the genesis and paleoenvironmental conditions during the regressive epochs of the Caspian Sea.

Structures attributed to cryogenic origin have been noted in the LVR by a number of researchers (Fedorov, 1957; Vasiliev, 1961; Moskvitin, 1962; Shkatova, 1975; Svitoch and Yanina, 1997). However, there are almost no data on the existence of permafrost during the late Pleistocene in this area, nor are detailed interpretations of the paleoenvironmental conditions for periods of formation and the development of the structures available. The cryostructures themselves mainly consist of permafrost "pots," thermal-contraction cracks and pseudomorphs along melted underground ice. Vasiliev (1961) describes the presence

of cryogenic structures (pseudomorphs, folded deformations, and involutions) in sections of Srednyaya Akhtuba, Chernyy Yar, Raygorod, Kopanovka, and others, classifying them as evidence of former permafrost conditions. Moskvitin (1962) also briefly mentioned the permafrost phenomena in sections of Quaternary formations of the Northern Caspian, without interpreting their genesis and conditions of their formation. A detailed description of the structure of the Atelian formation based on sedimentological, faunal, and pollen analyses was presented by Shkatova (1975). She also published drawings and photos of cryogenic structures in several sections (thermal-contraction cracks/wedge-shaped structures and involutions).

The cryostructures in the LVR are associated with the Atelian formation first identified by Pavel Pravoslavlev at the beginning of the twentieth century. The formation of the Atelian sediments took place gradually with the separation of the Lower Volga valley from the waters of the Caspian Sea. The Atelian formation is mainly represented by the loess–paleosol series (Költringer et al., 2021b). Loess as a continental archive of the Pleistocene history is of great interest in the northern Caspian, because it records paleoenvironmental conditions during the late Pleistocene. Indeed, loess deposits are widespread within the periglacial zone of the EEP and form detailed archives of changing environmental and sedimentary transport conditions (Velichko, 1973; Költringer et al., 2022).

As a result of the work of an international group of researchers in the LVR, a series of sections containing significant loess–paleosol sequences were described and analyzed, and data on the age and genesis of these deposits were obtained (Lebedeva et al., 2018; Költringer et al., 2021b, 2022; Taratunina et al., 2021, 2022; Kurbanov et al., 2022). Here we combine these new findings and first reports on cryogenesis in the region (Taratunina et al., 2021) with detailed interpretation of the cryostratigraphy of these sequences.

Materials and Methods

Field studies

This work is based on the results of a study of four reference sections of the Lower Volga valley (Fig. 1): Srednyaya Akhtuba, Leninsk, and Bataevka were studied on the left bank of the valley, and Raygorod on the right bank. All four sections reveal the typical stratigraphic sequence preserved on the lower Khvalynian Plain of the northern Caspian Lowland: the reference horizon of chocolate clays of the Khvalynian transgression, the polyfacies sequence of the Atelian subaerial formation, and the complex of sediments associated with the Khazarian transgressive stage of the Caspian Sea (∼MIS 5) (Fig. 2). In the northern part of the study area, subaerial deposits predominate in terms of thickness. Structures like pseudomorphs and involutions are found at different levels here.

Pseudomorphs in this paper are understood to be secondary structures resulting from the replacement of one sediment by another while retaining the external forms of the original material. According to this definition, these include the structures we are studying, which were formed as a result of ice melting and wedge filling with overlying material.

The fieldwork included reconnaissance studies, opening of cryogenic structures, their detailed description, sampling for laboratory studies, geodetic referencing of horizon boundaries and sampling points.
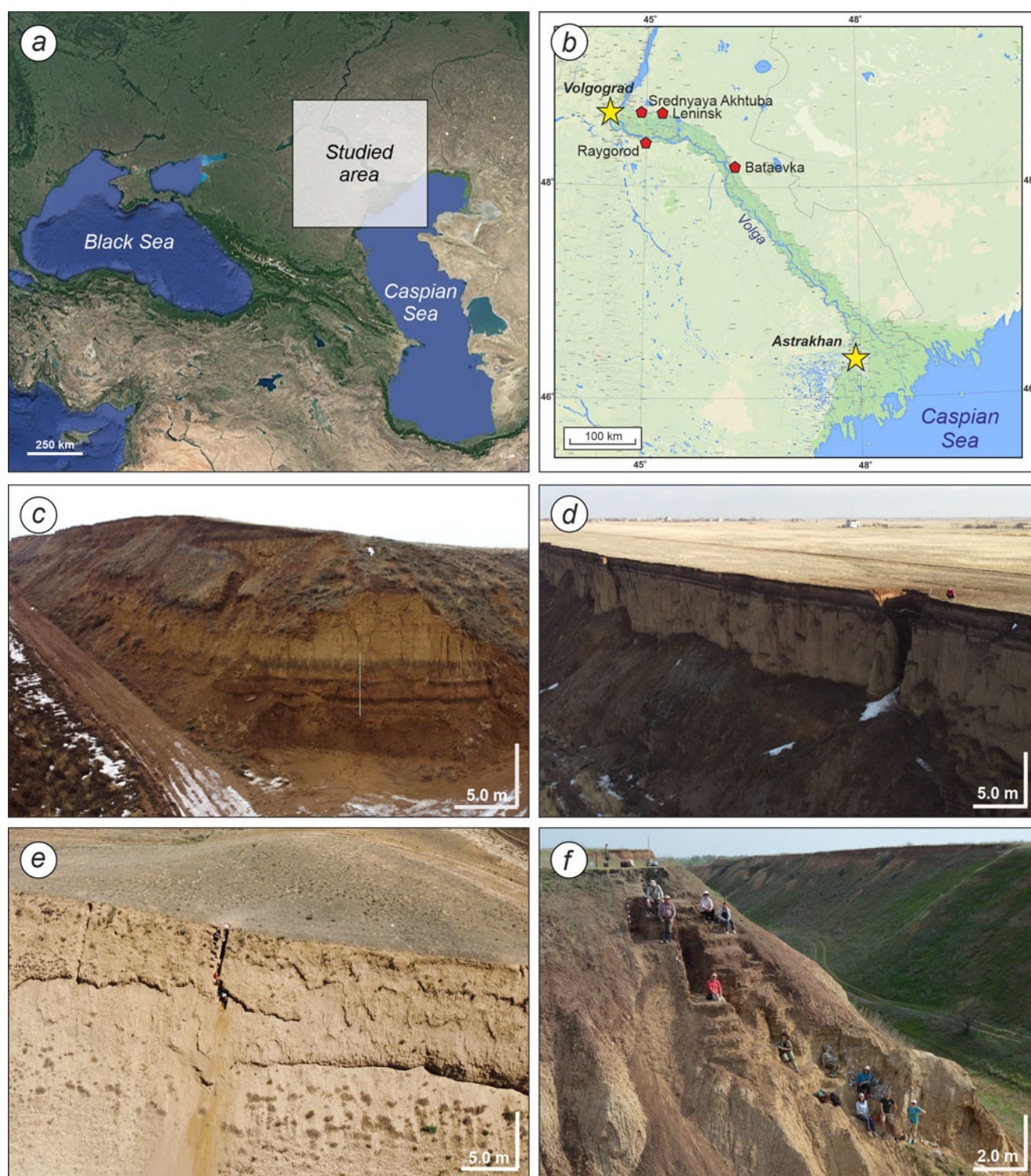
Figure 1. Studied area: (**a**) location of the studied area (Google Maps); (**b**) Lower Volga Region map with the locations of the studied sections; (**c–f**) general views of the Srednyaya Akhtuba (**c**), Raygorod (**d**), Bataevka (**e**), and Leninsk (**f**) sections.

Analytical studies

Laboratory studies included a description of the mineralogical composition of the deposits and a calculation of the Cryogenic Weathering Index (CWI), morphoscopy of quartz grains, micromorphology of the sediments, and absolute dating using optically stimulated luminescence (OSL).

Micromorphology

Microstructure of cryofeatures was studied using a TM 3000 scanning electron microscope (Hitachi) in combination with a Swift 3000 energy-dispersive spectrometer, and included two aspects:

1. Study of the microstructure of small-size monoliths (0.5–1.0 cm^3). Sample preparation was performed by splitting the
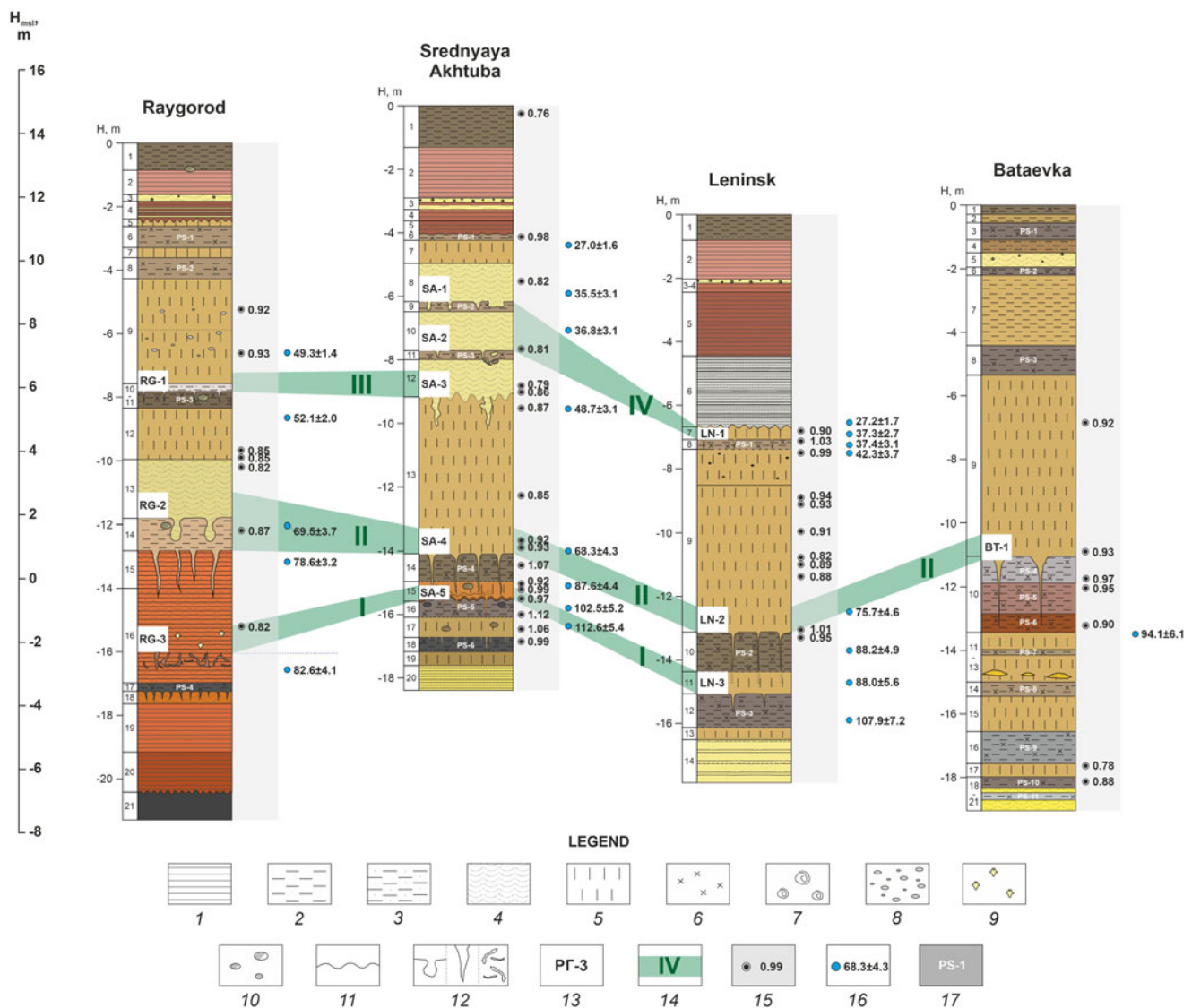
Figure 2. Correlation of the studied sections in the Lower Volga Region and stages of cryogenesis in the late Pleistocene. Legend: (1) clay; (2) loam; (3) sandy loam; (4) sand; (5) loess; (6) paleosols; (7) malacofauna; (8) carbonate concretions; (9) gypsum roses; (10) krotovinas; (11) erosion boundary; (12) cryogenic structures; (13) cryogenic horizons; (14) stages of cryogenesis; (15) Cryogenic Weathering Index; (16) luminescence ages, ka; (17) paleosol. Layers are marked on the left of the stratigraphic column; the colors of the deposits reflect the natural color of the sediment.

sample into two parts, with the back side of the sample glued to the slide, and following the standard procedure for preparing samples for examination in a scanning electron microscope (Kurchatova and Rogov, 2020).

2. Study of the microtextural characteristics of the surface of quartz grains, which carry information about the sedimentation conditions (Krinsley and Doornkamp, 1973; Vos et al., 2014; Woronko and Pisarska-Jamrozy, 2015; Kalinska-Nartiša et al., 2017). The samples were examined using scanning electron microscopy (SEM). Special attention was paid to the shape of the grains, surface topography, the presence of chips, the structure of aggregates, and organic and mineral inclusions.

Mineralogy and CWI

The CWI, which characterizes the relative degree of cryogenic weathering in the formation of deposits, was used to reconstruct the conditions of permafrost development in the region. To calculate this coefficient, a mineralogical analysis of two fractions is performed: fine sand (0.05–0.1 mm) and coarse silt (0.01–0.05 mm), as the main rock-forming minerals (quartz and feldspar) accumulate in these fractions in cryogenic conditions. The CWI is calculated by the formula: $CWI = (Q_1/F_1)/(Q_2/F_2)$, where Q_1 and F_1 are the content of quartz and feldspar in the 0.05–0.01 mm fraction, respectively; and Q_2 and F_2 are the content of quartz and feldspar in the 0.1–0.05 mm fraction, respectively (Konischev, 1981; Konischev and Rogov, 1994).

The mineralogical composition was determined using an X-ray diffractometer D2 PHASER (Bruker). The interpretation of X-ray patterns was carried out using the DiffracEva and DiffracTopas programs. According to the founder of this method, Konishchev (1999; Konischev et al., 2005), the values of the coefficient also allow correlation with the mean annual temperature on the soil surface.

Absolute dating

Luminescence dating obtained by the research group as part of this study was used to create a reliable basis for chronostratigraphic correlations for the studied sections. The first dating results for the deposits of the LVR by OSL methods were published for the Srednyaya Akhtuba section (11 ages; Yanina et al., 2017), and further OSL and IRSL dating details and luminescence characteristics of the samples were also published for Leninsk (39 ages; Kurbanov et al., 2022) and Raygorod (35 ages; Taratunina et al., 2022). As the ages were published previously, we provide here only a brief summary of the approach and refer the reader to the relevant original publications for more detail. Sampling took place at night in light-tight black bags or plastic pipes after preliminary cleaning of the sampling site. Chemical preparation of samples was carried out according to the standard procedure (Murray et al., 2021) for separation of quartz and K-feldspar of 90–180 and 180–250 μm grain size (see Kurbanov et al., 2022; Taratunina et al., 2022).

The luminescence signals of quartz and K-feldspars were examined using a TL/OSL Risø DA20 reader. Standard tests were carried out for the deposits of these sections: a "purity test," an assessment of the equivalent dose, and a dose-recovery test. The equivalent dose measurements for quartz were performed according to the standard SAR protocol (Kurbanov et al., 2022; Taratunina et al., 2022); a modified pIR IRSL (pIRIR) SAR protocol was used for K-feldspar (Buylaert et al., 2012). This made it possible to compare the final ages for quartz and K-feldspars and estimate the degree of bleaching before the burial of the sediment (Murray et al., 2012). The radionuclide concentration was measured using high-resolution gamma-spectrometry (Murray et al., 1987). Detailed information on the luminescence characteristics of the deposits and the results of dating can be found in thematic papers on the Raygorod (Taratunina et al., 2022) and Leninsk (Kurbanov et al., 2022) sequences.

Results

Section lithostratigraphy and characteristics of the cryogenic structures

The Srednyaya Akhtuba section is located 500 m east of the village of Srednyaya Akhtuba (SA; Height above mean sea level [H_{amsl}] 14.9 m, 48°42′01″N, 44°53′37″E; Fig. 2). This section is located in a ravine that cuts through the surface of the Khvalynian terrace. The section is 20 m thick and characterizes the structure of deposits accumulated during the Atelian regression of the Caspian Sea, as well as the thick layer of "chocolate clays" of the Khvalynian transgression. The polyfacies sequence of sediments is described here (from top to bottom, here and later): (1) modern soil (kashtanozem soil, layer 1); (2) horizon of chocolate clays (layers 2–5); (3) alluvial sands with weakly developed paleosols (layers 6–12); (4) a thick horizon of loess deposits, the upper part of which is eroded (layer 13); (5) alternation of loess and three developed paleosols (layers 14–19); and (6) lacustrine–estuarine sediments (layer 20). The description of the section, its stratification, and the results of luminescence dating are presented by Yanina et al. (2017).

A unique feature of the Srednyaya Akhtuba section is the pronounced late Pleistocene cryogenesis visible at the site: traces of five horizons with cryogenic structures in the form of involutions and pseudomorphs are found in this section (Figs. 3 and 4).

The first (from top to bottom) horizon with traces of cryogenic structures (SA-1) occurs at a depth of ~6.2 m in the form of pseudomorphs in layer 9. Structures of different shapes and vertical thicknesses (20–30 cm) were identified within the outcrop: funnel-shaped with an extension at the end, wedge-shaped with a rounded end; some structures with horizontal planes and toothed edges (Fig. 3a and b).

At a depth of 7.7 m, the second horizon with cryogenic structures (SA-2) was observed. SA-2 is represented by a series of rounded tuber-like forms (Fig. 3c), dissecting paleosol PS-3 and penetrating into the underlying alluvial horizon. The infilling material is represented by fine-grained sand of a brown and gray-yellow color. The central parts of these formations are weakly ferruginated; part of them, enclosed in the paleosol, have rounded borders. Structures penetrating the alluvial horizon (layer 10) have a wedge-shaped tail.

The third horizon (SA-3) is situated on the top of the loess stratum (layer 13) at a depth of 9.1 m. Here, a layer of medium-grained sand with horizontal bedding is replaced by a dense pale-yellow loess along the erosional boundary. The loess sequence, with a total thickness of 5.0 m, includes in the upper part a number of large pseudomorphs. A two-level cryogenic structure was found in the section (Fig. 3d): the upper, wider part is a bag-like pocket 70–75 cm deep, up to 40 cm wide, filled with heterogeneous loose sand of dark beige color, with layering that indicates a gradual filling of the structure from the edges to the center; the lower part of the pseudomorph is represented by a wedge-shaped tail up to 20 cm wide, with a vertical length of 35–40 cm. The boundary between the pseudomorph and the host material is uneven, with numerous eddies and folds, accentuated by a thin line of carbonates.

The structures of the fourth cryogenic horizon of Srednyaya Akhtuba (SA-4, depth 14.1 m) are clearly recorded in paleosol PS-4 (layer 14) in the form of wedge-shaped pseudomorphs (Fig. 3e). The width of the structures in the upper part is 12–20 cm, and the vertical extent is from 0.6 to 1.0 m. The distance between wedges is 40–60 cm, observed regularly in the outcrop. The wedge-shaped structures are filled with overlying loess material. The enclosing deposits are characterized by a reticulate texture, presumably of cryogenic origin (Makeev et al., 2021).

Traces of the fifth horizon (SA-5, depth 15.5 m) were recorded in paleosol PS-5 (layer 16) in the lower part of the section (Fig. 4a). They are expressed as thin wedge-shaped pseudomorphs that cut the underlying loess (layer 17) and cross the surface of the lowermost paleosol PS-6 (layer 18) with small tails. The wedges have a relatively wide bell at the top (12–20 cm), quickly narrow, and continue in the form of tails, sometimes breaking up into two to three separate endings. The height of the wedge-shaped structures is from 0.8 to 1.5 m; the distance between the wedges is 40–60 cm. The structures are filled with lighter loess material from layer 15. The boundary of layers 15 and 16 is broken by uneven toothed contacts (Fig. 3f). The tail parts of the structures of SA-5 cut the surface of the underlying PS-6, layer 18 (Fig. 3g).

The Raygorod section (RG; H_{amsl} 13.7 m, 48°25′53″N, 44°58′02″E; Fig. 2) is located on the right bank of the Volga River, 1 km east of the village of Raygorod. The section is a stratotype of the Atelian deposits of the LVR (Svitoch and Yanina, 1997) and reveals the structure of the early Khvalynian terrace of the Caspian Sea. This sequence is represented by deposits of different facies with a total thickness of more than 21 m: (1) modern soil (layer 1); (2) chocolate clays stratum (layers 2–4); (3) thick
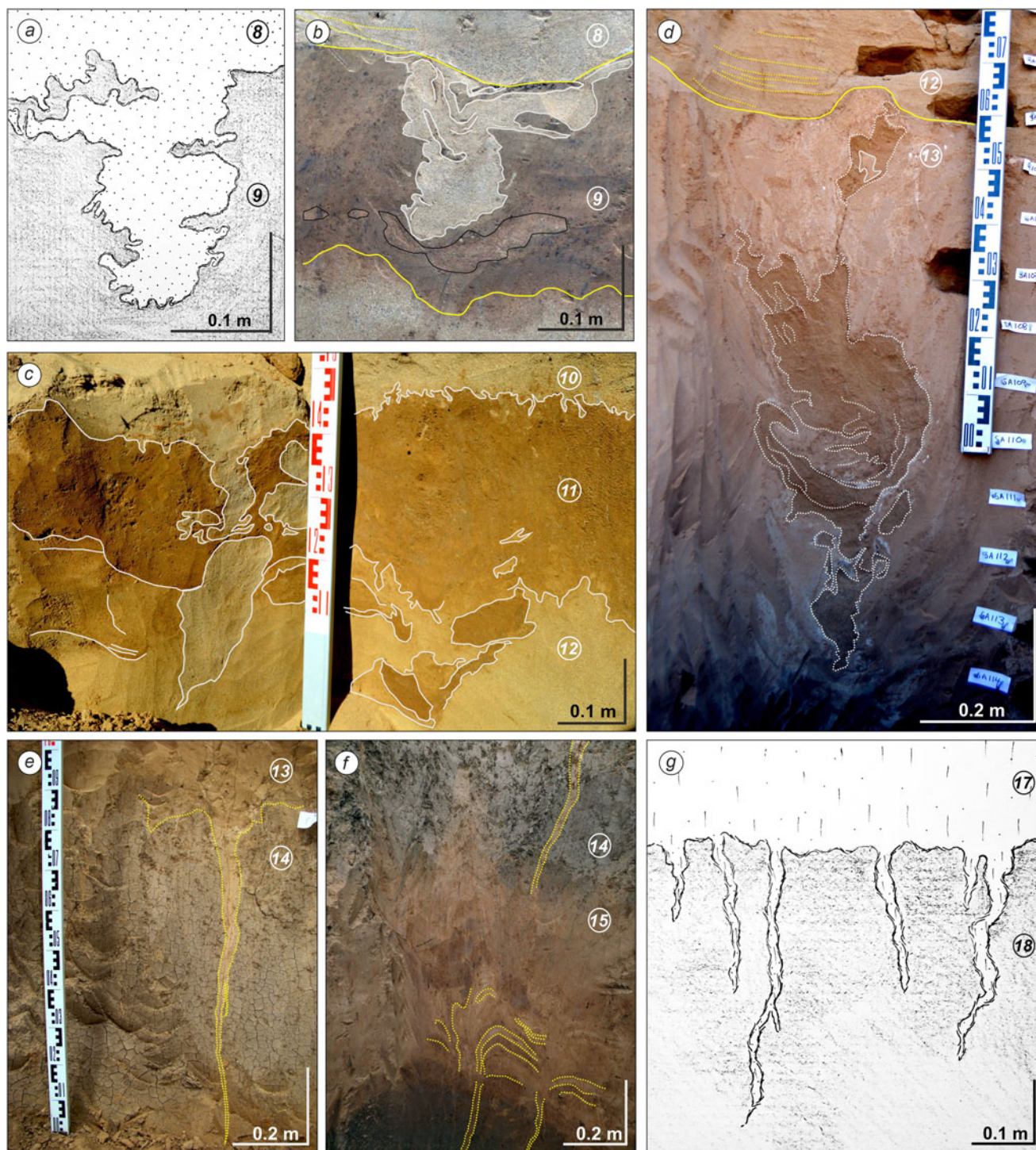
Figure 3. Cryogenic structures in the Srednyaya Akhtuba section: (**a and b**) wedge-shaped structures with horizontal processes of the first cryogenic horizon (SA-1); (**c**) involutions in alluvial deposits, the second cryogenic horizon (SA-2); (**d**) two-level cryogenic structure of the third cryogenic horizon (SA-3); (**e**) wedge-shaped structure in the paleosol (SA-4); (**f**) deformation in the structure of loess and paleosol at the boundary between layers 15 and 16, lower part (SA-5); (**g**) tail parts of the structures of SA-5 (sketch). Numbers in circles indicate the layer numbers from Fig. 2.

loess–paleosol stratum (layers 5–12); and (4) alluvial sediments (channel and floodplain facies) with traces of pedogenesis (layers 13–21).

Three cryogenic horizons were identified in the Raygorod section. The uppermost (RG-1, depth 7.9 m) is situated in a paleosol and represented by wedge-shaped pseudomorphs cutting layer 11

up to 25–30 cm vertically. They are located at a distance of 30–50 cm from each other. The width of the cryogenic structures along the top is 2–3 cm; the vertical width of the wedge is preserved and is 1–2 cm. The tails of the structures are not visible. The structures are poorly distinguishable and filled with overlying sandy loam of a pale color.
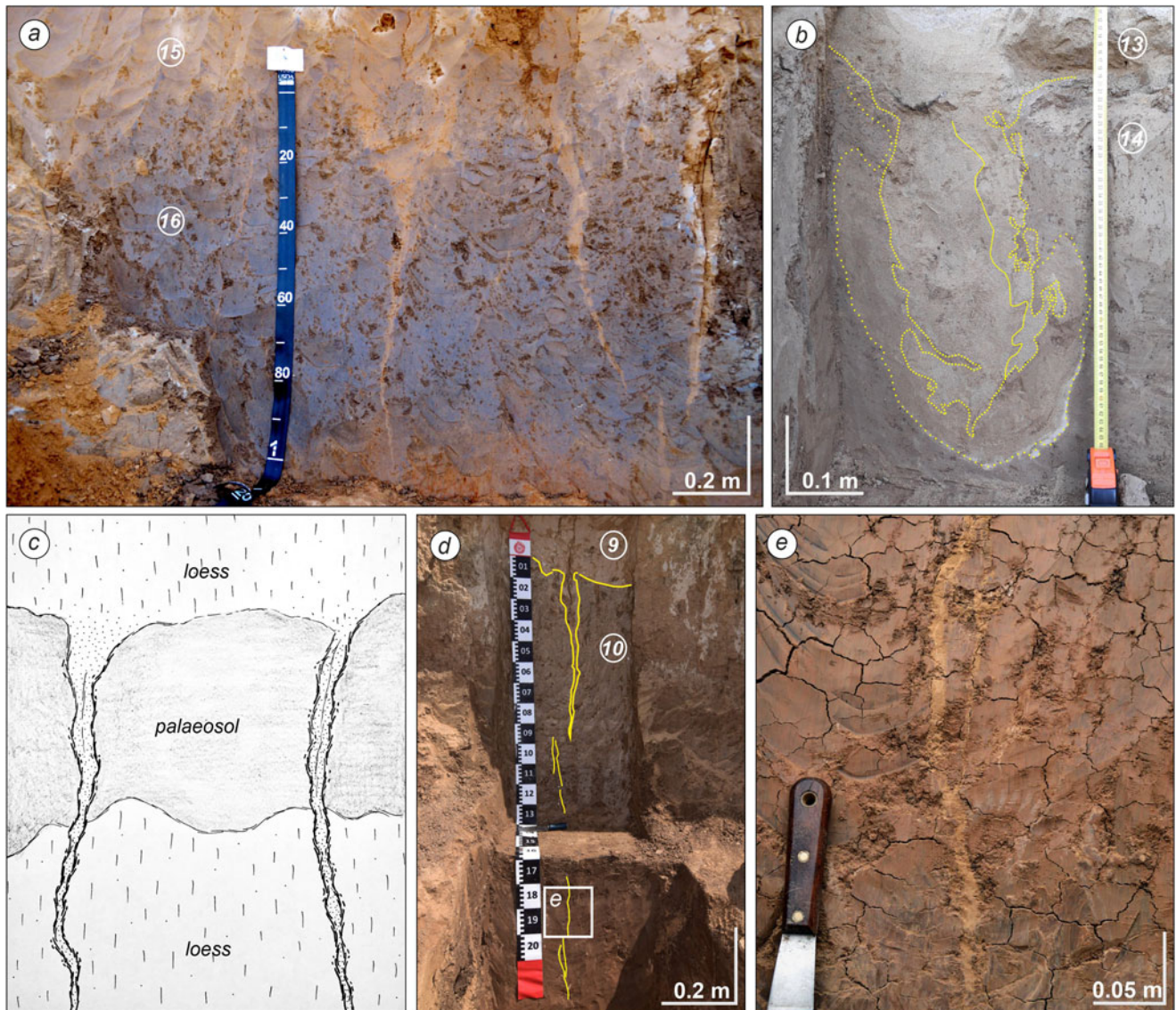
Figure 4. Cryogenic structures in the Lower Volga sections: (**a**) wedge-shaped structure in the paleosol (SA-5); (**b**) bag-like pseudomorph in alluvial deposits of the Raygorod section; (**c**) thin wedge-shaped forms filled with overlying loess material and cutting paleosol horizons, Leninsk section (sketch); (**d**) wedge-shaped structure in the Bataevka section; (**e**) reticulate texture in sediments and a thin cryogenic tail filled with loess material (enlarged fragment from **d**). Numbers in circles indicate the layer numbers from Fig. 2.

The second horizon (RG-2), located at a depth of 11.8 m, is represented by bag-like pseudomorphs in layer 14, with a vertical length of 50–60 cm, and filled with overlying alluvium. The studied structure of this horizon (shown in Figure 4b) is bag-shaped and embedded in non-layered grayish-brown loams with evenly distributed large isometric pores (1–3 mm). The vertical size of the structure is 55 cm; the width is from 20 cm at the top to 45 cm at the bottom. The outer contour of the structure is represented by light brown sandy loam, 5–10 cm thick; the interior of the pseudomorph is filled with light yellow sand. The structure is separated from the host deposits by a thin (0.1–0.3 cm) white boundary of carbonate crystals.

The third horizon in Raygorod (RG-3) was exposed in the lower part of the section at a depth of 16.0 m. It is up to 30 cm (vertically) and is represented by pale-yellow loam, penetrated by thin veins up to 1.5–2.0 cm wide and 25–30 cm long. In a horizontal cross section, the wedges are irregular lattices with

polygons 5–15 cm in diameter. The wedges have clear boundaries and broken shapes. The structures are filled with gray-brown loam enriched by organic matter. There is high content of gypsum nodules ranging from 1 to several mm in size.

The Leninsk section (LN; H_{amsl} 11.5 m, 48°43′17″N, E 45° 09′33″E; Fig. 2) is located 2 km west of the city of Leninsk (Volgograd region), in one of the large gullies on the left bank of the Akhtuba River. The structure of the section includes: (1) a modern soil (layer 1); (2) stratum of marine deposits—reference horizon of chocolate clays (layers 2–5); (3) underlying gray clay (layer 6); (4) thick layer of subaerial sediments (layers 7–13), represented by the alternation of loess and paleosols, which contain cryogenic structures in the form of wedge-shaped pseudomorphs; and (5) horizon of lacustrine–estuarine deposits exposed at the base of the section.

Three horizons with cryogenic structures were identified in Leninsk. The first one (LN-1) was identified at the boundary of

loess (layer 7) and paleosol (layer 8) and is represented by thin pseudomorphs that extend from the overlying pale-yellow loess into the underlying paleosol with a vertical length of 35–40 cm and width of 1.5–2.0 cm. The structures are irregularly shaped, and tails are not visible

The second horizon of cryogenic structures (LN-2) starts at the boundary between loess (layer 9) and paleosol (layer 10) and is represented by wedges with a vertical length of 65–70 cm in a sub-vertical direction (Fig. 4c). Wedges with branches, filled with overlying dense, heterogeneous, non-layered loess material, are located at a distance of ~60 cm from each other. The wedges change their vertical width from a few centimeters to 20 cm (average 5–7 cm). One of the wedges was described and sampled in detail.

The third cryogenic horizon at Leninsk (LN-3) also marks the loess–paleosol boundary (layers 11–12). The structures are thin wedge-shaped pseudomorphs up to 2–3 cm in thickness, crossing the paleosol to a depth of 30–40 cm. There are two types of wedges—those filled with loess sediments and those filled with darker soil material.

The Bataevka section (BT; H_{amsl} 11.7 m, 48°09′51″N, 46°17′14″E; Fig. 2) is located 15 km southeast of the city of Akhtubinsk, on the left bank of the Akhtuba River. The total thickness of the studied sequence is 19 m. This is the most southerly location with thick loess–paleosol sediments in the LVR. This section reveals sequences of marine and subaerial formations: (1) the upper part is an alternation of subaerial soil horizons and dense loess-like loams/sandy loams (layers 1–8), layer 5 being sands of Khvalynian transgression with shells of Caspian mollusks; (2) the middle part of the section is represented by a thick horizon of dense, calcified loess (layer 9), which is underlain by a pedocomplex (layer 10) with wedge-shaped structures (similar to the paleosol structures in the lower part of the Srednyaya Akhtuba and Leninsk sections); (3) below (layers 11–18) a frequent alternation of loess and paleosol horizons continues, the latter contains charcoal. The base of the section is represented by interbedded silts and fine sands (layers 19–21).

One cryogenic horizon was identified in this section (Fig. 4d and e). It is located at a depth of ~11.0–13.0 m and contains wedge-shaped pseudomorphs starting in the loess (layer 9) and cutting the underlying paleosols (layer 10). The horizon is represented by thin wedges with a vertical length of 2.0–2.5 m, located at a distance of 40–50 cm from each other. The wedges have a funnel-shaped socket (12–17 cm in cross section) and are filled with overlying loess material. The width of the main body is ~2 cm. At a depth of ~2.0 m, in the tail part, the structures gradually narrow, sometimes disappearing and reappearing as veins 1–3 mm wide, filled with lighter loess material. The boundaries of the wedges are clear, not linear, distinguished by color and infilling material, with numerous branches in the tail. Horizontal stripping of the tail revealed a polygonal grid with polygons up to 20 cm in size. The enclosing paleosol deposits have a reticulate texture, probably of cryogenic origin (Fig. 4e).

Lithology

Microstructure of the loess–paleosol stratum
The microstructure of deposits from the LVR was studied using SEM analysis (Fig. 5). Samples were undisturbed loess monoliths and separated quartz grains (sand and silt fractions). The microstructure mainly comprises large aggregates up to 3 mm, composed of particles of different sizes and degrees of aggregation:

from sharp-angled quartz particles of fine sand to fragmented cutans of various compositions (iron, silicon, calcium). A special feature of the microstructure is the presence of tubular pores (Fig. 5a) with a diameter up to 0.6 mm, with a compaction of the soil mass with silty particles on the walls. The cross section of the pores is close to a circle in most examples, but it has a hexagonal shape in some cases. In addition, radial cracks are often visible around the channels.

Morphology of particles of the sand fraction
The morphology of quartz particles (Fig. 5b–h) in the studied samples is very diverse and reflects the conditions of deposit formation in different environments. The host alluvial deposits are characterized by both well-rounded, isometric grains with shallow surface pits and well-rounded, irregularly shaped grains (Fig. 5b). There are also angular grains with smoothed edges. Quartz grains from loess horizons have conchoidal fractures and lamellar chips (Fig. 5c), sometimes smoothed by silica dissolution and reprecipitation. There are grains that have probably undergone eolian processing: numerous pits are unevenly distributed on the surface of a well-rounded grain (Fig. 5d). Well-rounded grains with evidence of high-energy transport effects of water—irregular V-shaped depressions—were also found (see Fig. 5e). Quartz grains from the material of pseudomorphs and host sediments of the sections were studied. The infilling material of the tail part of the structure is characterized by angular grains (Fig. 5f). Quartz grains also showed numerous conchoidal fractures both in the host sediments (Fig. 5g) and in the fill of structures (especially in the tail part) (Fig. 5h).

Morphology of aggregates of the silt fraction (0.05–0.005 mm)
Loess consists of structural units of various sizes, from microscopic aggregates to well-defined columnar units. When studying the microstructure, special attention was paid to aggregates of the silt fraction (microaggregates), because a number of researchers point to their cryogenic origin (Popov, 1960, 1967; Konishchev, 1981; Zhai et al., 2021).

The material of loess layers contains aggregates of various sizes and structures. Large and loose aggregates (0.5–0.1 mm) are usually composed of tens of particles of the silt fraction. Smaller aggregates are dominated by fine silt and clay particles. Intra-aggregate pores are smaller and flattened. Most of the aggregates are formed by silty and clay particles connected by iron-carbonate cement (Fig. 5i). The aggregates are solid and are not destroyed when washed with water and exposed to ultrasound. Contact between the aggregates occurs through clay "bridges" that form intra-aggregate pores of 0.01–0.005 mm.

Authigenic minerals in all sections are represented by a "fur coat" and "needles" of calcium carbonate on the surface of mineral particles (Fig. 5j) as well as gypsum inclusions (Fig. 5k). Iron is represented by amorphous films on the surface of particles, siderite concretions, and rare forms of magnetite and titanomagnetite (Fig. 5l). Witherite crystals are also found. The composition of authigenic minerals indicates cryo-arid conditions for the formation of loess horizons in sections of the LVR.

CWI
To assess the impact of cryogenesis on the deposits, the mineralogy of the main granulometric fractions of loess (fine sand and coarse silt) was analyzed, and the CWI was calculated. The CWI values for the Srednyaya Akhtuba section fluctuate in a fairly wide range: they record both horizons that formed in cold
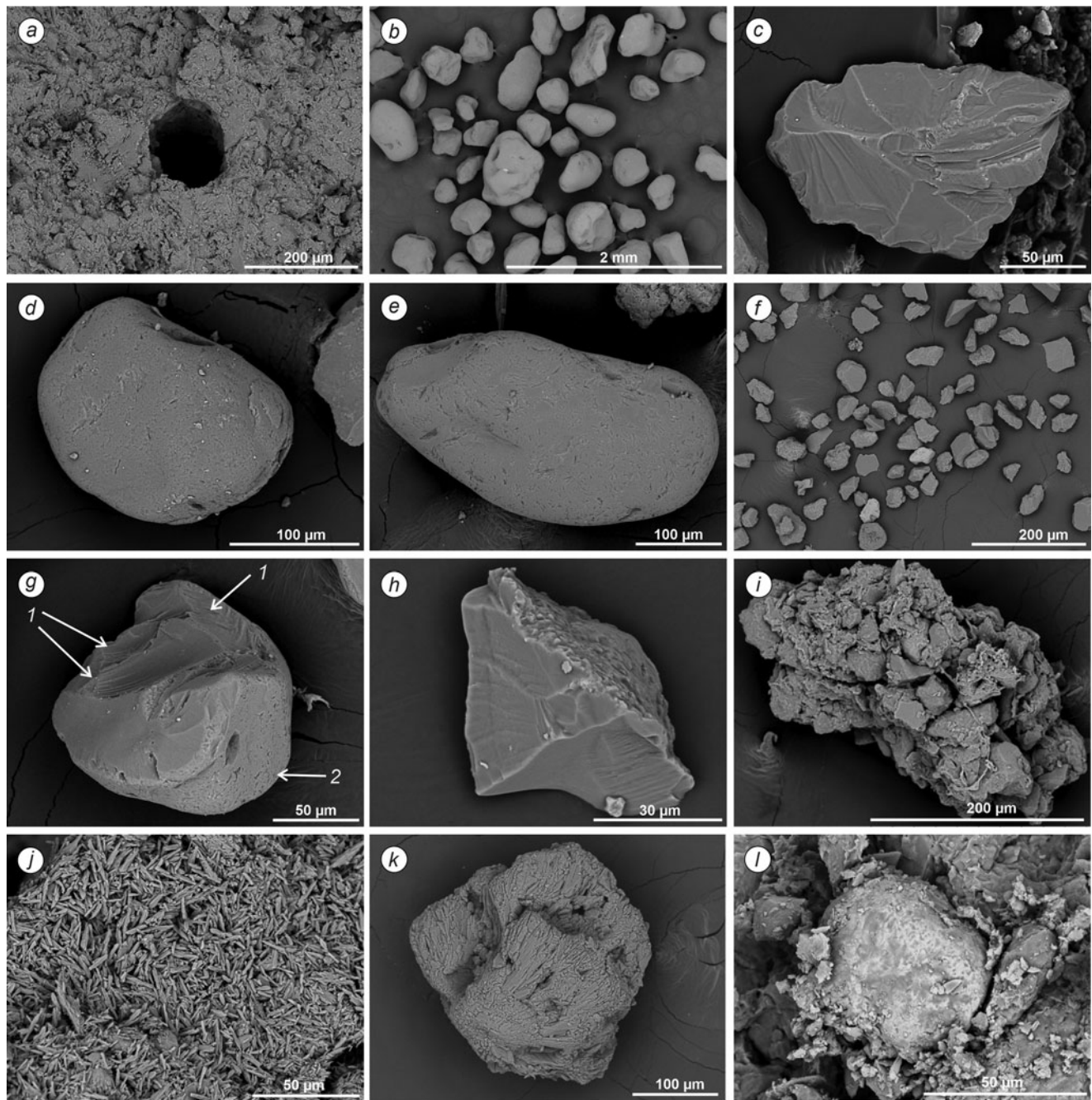
Figure 5. Microstructure of sediments and particle morphology: (**a**) tubular pore in loess microstructure (Bataevka section, layer 9, depth 10.9 m); (**b**) overview under a smaller magnification, grains of alluvial horizon (Srednyaya Akhtuba section, layer 10, depth 7.6 m); (**c**) angular grain with numerous chips on the surface (Leninsk section, filler of the tail part of the ice wedge cast, cryogenic horizon LN-2); (**d**) isometric grain with irregularly distributed pits on the surface (presumably of eolian environment) (Srednyaya Akhtuba section, layer 13, depth 14.0 m); (**e**) irregular V-shaped depressions on well-rounded grain (Leninsk section, layer 12, depth 15.7 m); (**f**) overview under a smaller magnification, angular grains (Leninsk section, filler of the tail part of the ice wedge cast, cryogenic horizon LN-2); (**g**) grain with fresh conchoidal fractures (1) and a surface that has retained its original roundness (2) (the same location); (**h**) angular grain with numerous chips on the surface (Leninsk section, filler of the tail part of the ice wedge cast, cryogenic horizon LN-2); (**i**) an aggregate composed of particles of different size (Srednyaya Akhtuba section, depth 14.0 m); (**j**) needle-shaped calcite (Raygorod section, cryogenic horizon RG-3, depth 16.2 m); (**k**) gypsum in sediments containing cryogenic structures (Leninsk section, cryogenic horizon LN-2, depth 13.1 m); (**l**) titanium-ferruginous nodules (Srednyaya Akhtuba section, depth 15.6 m).

climatic conditions and those that do not have visible traces of such conditions (see Fig. 2). The CWI value in the Holocene deposits (layers 2 and 1) is 0.76, which corresponds to warm conditions. The accumulation of the alluvial stratum corresponds to the second half of MIS 3 and the early phase of the early Khvalynian transgression of the Caspian Sea (layers 8–12),

characterized by low CWI values (0.79–0.82). In the layers formed during the Atelian regression, the CWI values are higher: 0.87–0.93 for layer 13. In the composition and structure of the deposits corresponding to the end of the late Khazarian transgressive stage (~MIS 5), the impact of cooling is clearly traced: according to the CWI calculations, the most affected layers are 14 (MIS 5a, CWI

1.07), 16 (MIS 5c, CWI 1.12), and 17 (MIS 5d, CWI 1.06). These horizons were probably subjected to cryogenic transformation in cold conditions of MIS 5b and MIS 4 during a time of permafrost in the studied area. In the Bataevka section, for the lower part of the loess sequence at the boundary of layers 9 and 10, a value of 0.93 was obtained, which indicates severe conditions for the beginning of loess formation. Below, in the pedocomplex, the CWI is 0.97 and decreases along the profile of paleosols to 0.90. The CWI values of the Raygorod section are calculated for the loess and alluvial layers. In both cases, the CWI values do not exceed 1, although the CWI in loess is higher at 0.85–0.93 versus 0.82–0.87 in alluvium. The CWI values in the loess strata of Leninsk (layer 9) vary from 0.82 to 0.99, which reflects changing moisture conditions—higher CWI values for a monotonous loess stratum indicate a more intense period of cryogenic processes. For paleosol horizons, the CWI is maximal at the loess/paleosol boundary: 1.03 at the boundary of layers 7/8 (LN-1) and 1.01 at the boundary of layers 9/10 (LN-2). In Leninsk, a more detailed assessment of the CWI was carried out: material for analysis was taken from the infilling of the pseudomorph of the second cryogenic horizon (5 samples) and from the enclosing deposits (8 samples). The differences in the CWI values for the enclosing and infilling material are not large, but a pattern is observed: in the paleosol deposits of layer 10, the coefficient is higher (0.88–1.05), compared with the overlying layer 9 (0.76–0.90).

Luminescence dating

Twenty-two ages were obtained by luminescence dating from layers containing cryogenic features in Bataevka, Srednyaya Akhtuba (Yanina et al., 2017), Leninsk (Kurbanov et al., 2022), and Raygorod (Taratunina et al., 2022) (Fig. 2). Detailed characteristics, tests, and dating results are presented in Kurbanov et al. (2022) and Taratunina et al. (2022), quartz OSL signals of sand-sized grains from all samples are sensitive and dominated by the fast component. The completeness of bleaching of these deposits is demonstrated by the good agreement between the younger quartz OSL ages and the $pIRIR_{200,290}$ ages, and resulting ages pass internal tests. Thus, the luminescence data allow detailed age depth analysis of the sections here, and combined with the analyses presented earlier, allow characterization of four main stages of the development of cryogenesis in the LVR during the late Pleistocene (Fig. 2, Table 1). Chronological data used for the correlation of studied sections are summarized in Table 1; in Figure 6, the cryogenic stages identified here for the Lower Volga are correlated with events on the EEP and in the Caspian region.

Stages of cryogenesis in the LVR

The concepts of "cryogenic horizon" and "cryogenic stage" in this work are understood differently: cryogenic horizon is a geologic body that bears traces of cryogenesis, that is, a layer with cryogenic structures; the cryogenic stage is the time of formation of cryogenic structures.

The beginning of stage I occurs at the end of MIS 5c and in the first half of MIS 5b (95–90 ka). For this period, various structures were identified, the formation of which is associated with subaerial conditions (Srednyaya Akhtuba, Leninsk). Here, in the interfluve position, large wedge-shaped pseudomorphs with a length of up to 1.5 m were formed. In addition, in coeval floodplain deposits (Raygorod section), where freezing occurred to a shallow depth, smaller pseudomorphs formed thin vertical wedges (the

RG-3 cryogenic horizon) up to 30 cm long. The maximum CWI value in this stage is 1.12.

Stage II of cryogenesis in the LVR occurred ~75–70 ka and corresponds to the transition period from MIS 5a to MIS 4. Structures of different shapes were recorded for this time period in different sediment types: (1) in the Leninsk (LN-2), Srednyaya Akhtuba (SA-4), and Bataevka (BT-1) sections, wedge-shaped pseudomorphs with a vertical length of ~0.6–2.0 m were recorded in subaerial loess–paleosol deposits; and (2) in the Raygorod section (RG-2), structures of a different form are present, enclosed in silty alluvial facies—bag-like pseudomorphs 55–60 cm high and 20–50 cm wide, with layer-by-layer filling with overlying alluvial material.

The cryogenic structures of this stage, found in Srednyaya Akhtuba, Leninsk, and Bataevka, are enclosed in subaerial loess–paleosol deposits and all have a similar structure and parameters, although they are located at different latitudes. However, the structures in the Raygorod section, located at the same latitude as the Srednyaya Akhtuba, are enclosed in alluvial deposits and have a different morphology. This indicates that the form of the structures depends on the origins of the deposits rather than their position within one region.

The beginning of stage III corresponds to MIS 3c, extending to the first half of MIS 3b (~52–45 ka). This stage is marked in Raygorod (RG-1) at a depth of ~7.7 m as wedge-shaped pseudomorphs represented by thin structures up to 30 cm high; the width of the structures is continuous vertically. They cut a weakly developed paleosol and are filled with overlying loess material. The tails of the structures are not visible. The structures are developed in loess–paleosol subaerial deposits formed under watershed conditions with low moisture content. In the Srednyaya Akhtuba section, pseudomorphs up to 1.5 m long with a two-level structure (SA-3) are observed: the wide upper part is a bag-like pocket, 70–75 cm deep, up to 40 cm wide, filled with heterogeneous loose sand; the lower part is represented by a wedge-shaped tail up to 20 cm wide, with a vertical length of 35–40 cm. The boundaries of the pseudomorphs and host material are uneven, with numerous eddies and folds.

Stage IV corresponds to MIS 3a (37–35 ka). In the LVR, this stage is expressed in the Leninsk section, as well as in two levels in Srednyaya Akhtuba: (1) The lower level in the Srednyaya Akhtuba section (SA-2) is represented by involutions, which disturb the uniformity of deposits of floodplain soils and the alluvial layers. (2) The upper horizon (SA-1) is represented by pseudomorphs of various morphology—wedge-shaped structures, forms with horizontal lenses; all structures of this horizon are characterized by a small thickness (up to 25 cm) within the paleosol horizon and clear boundaries with enclosing deposits. (3) In Leninsk (LN-1), wedge-shaped pseudomorphs of a small size (up to 30 cm vertically) were recorded for this stage. They are expressed throughout the thickness of the underdeveloped paleosol and are filled with overlying loess material. These structures were formed in subaerial watershed conditions.

Discussion

Evidence for permafrost in the LVR

The cryogenic origin of the structures exposed in the sections is confirmed by both field and laboratory studies. The morphology of the structures and the features of their relations with enclosing and overlying material indicate the cryogenic nature of their

Table 1. Stages of cryogenesis and types of cryogenic forms in the studied sections of Lower Volga valley.

Stage	Section (cryogenic horizon)	Type of cryogenic structures	H^a_{amsl} (m)	Age (ka)	The conditions for the formation of structures in various deposits
I MIS 5b	Srednyaya Akhtuba (SA-5)	Thin wedge-shaped structures up to 1.5 m	−0.64	~95–90	Subaerial deposits; dry, cold conditions
	Leninsk (LN-3)		−1.73	~95	
	Raygorod (RG-3)	Thin structures up to 30 cm	−2.35	~90	Floodplain deposits; wet, cold conditions; seasonal freezing
II MIS 5a/MIS 4	Leninsk (LN-2)	Thin wedge-shaped structures up to 1.0 m	−2.10	~75	Subaerial deposits; dry, cold conditions; permafrost
	Raygorod (RG-2)	Bag-like pseudomorph with layer filling	1.87	~75	Alluvial deposits; wet conditions; deep thawing
	Srednyaya Akhtuba (SA-4)	Thin wedge-shaped structures up to 1.0 m	0.74	~70	Subaerial deposits; dry, cold conditions; permafrost
	Bataevka (BT-1)	Thin wedge-shaped structures up to 2.5 m	0.72	~70	Subaerial deposits; dry, cold conditions; permafrost
III MIS 3b/c	Raygorod (RG-1)	Thin wedge-shaped structures up to 30 cm	6.12	~52–50	Subaerial deposits; dry, cold conditions
	Srednyaya Akhtuba (SA-3)	Two-level pseudomorph up to 1.5 m with layer filling	5.74	~45	Alluvial deposits; wet conditions; rise of the Volga level; deep thawing
IV MIS 3a	Leninsk (LN-1)	Thin wedge-shaped structures up to 30 cm	4.32	~37–35	Subaerial deposits; dry, cold conditions; permafrost
	Srednyaya Akhtuba (SA-2)	Involutions	7.16	~37	Development of floodplain soils in alluvial sediments; wet conditions; permafrost
	Srednyaya Akhtuba (SA-1)	Thin wedge-shaped structures up to 25 cm	8.36	~35	Development of floodplain soils in alluvial sediments; wet conditions; seasonal freezing

a H_{amsl}, height above mean sea level.
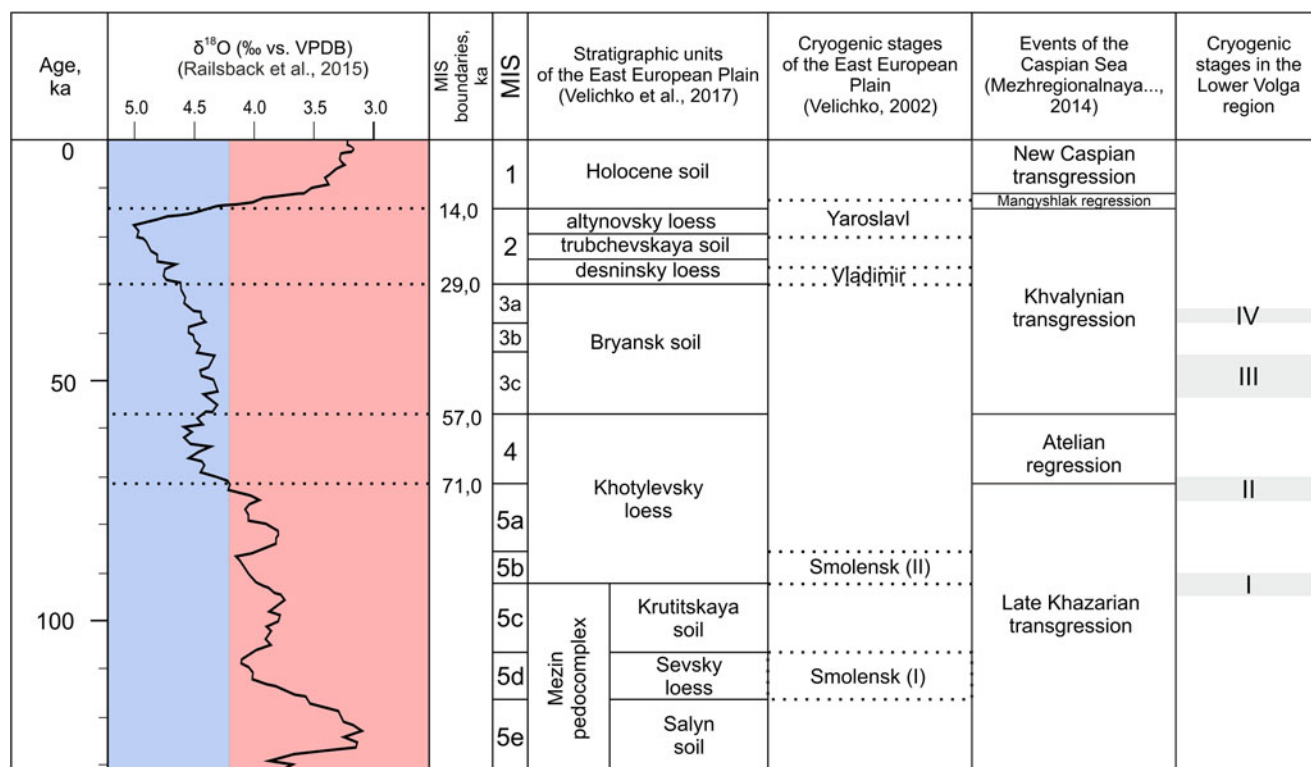
Figure 6. Correlation of cryogenic events in the East European Plain and the Lower Volga Region. Sources: Velichko, 2002; VSEGEI, 2014; Railsback et al., 2015; Velichko et al., 2017.

formation: clear boundaries (Fig. 3), filling with overlying material (Fig. 3a–c, e, and g), disturbances along the upper boundary of the structures (Fig. 3d), a wider upper part of the structures (Figs. 3d and 4b and c), bending of the host deposits at the boundary of the structures and the hosting layers (Fig. 3f), and segregation lenses (Fig. 3a and b). Indeed, when studying sections of Upper Pleistocene deposits of the LVR, previous researchers have repeatedly observed various structures for which a cryogenic origin was assumed (Vasiliev, 1961; Moskvitin, 1962; Shkatova, 1975). Remarkably, our results indicate that permafrost conditions already occurred in the LVR, in the south of the widely assumed Eurasian last glacial permafrost belt, by the end of MIS 5 and episodically into late MIS 3, after which the Khvalynian transgression of the Caspian Sea removed evidence for any later phases. Given that these features are widespread, coupled with the relatively flat terrain, we argue that these episodes likely reflect phases of continuous permafrost development in the area, and thus suggest that mean annual soil temperatures dropped below −5°C. Evidence for extreme aridity in the area (Költringer et al., 2021a, 2021b) during most of the time of deposition of the subaerial sediments suggests that the LVR experienced a highly continental climate, likely with extremely cold and arid winter conditions.

The cryostructures in the studied area are found in three deposit types that differ in genesis: various types of alluvium, paleosol, and loess horizons. In each of these sediment types, cryogenic features differ both in scale and the shape of structures. We associate the diversity of cryogenic structure morphology with: (1) different composition and particle-size distribution of sediments; (2) different water content in sediments both at the time of sedimentation formation and subsequent freezing and at the time of ice melting; and (3) the climate conditions in the region during various stages of the Late Quaternary, which influenced the active-layer depth and the type of permafrost (continuous/sporadic). The sediments enclosing cryogenic structures are predominantly paleosols, which are characterized by a more clayey composition and, consequently, are more waterlogged. In dry loess, cryogenic features are reflected in the vertical separation of loess and its block structure (Feng et al., 2021). The cryogenesis of the LVR also has specific features arising from arid conditions (Figs. 3e and g and 4a, c, and d), its relatively southerly location, and the impact of the transgressive–regressive history of the Caspian Sea (Fig. 3d) and the evolution of the Volga River (Figs. 3d and 4b).

The results obtained from laboratory studies also confirm the cryogenic origin of the structures shown in sections. For deposits of cryogenic horizons and individual structures within them, a detailed calculation of the CWI was carried out, which showed that the host paleosols are characterized by higher CWI values (1.07, 1.12), which decrease along the profile with depth. This is logical, because sediments from higher layers go through more freeze–thaw cycles, which means they experience more intense cryogenic transformation. Despite the fact that the loess horizons were formed during the cold stages, they are characterized by lower CWI values (0.90–0.99), which again confirms that the conditions were arid at the time of their formation, probably indicating a much shallower active layer and only the surface being affected by seasonal thawing with little cryogenic transformation.

It is believed that the nature of surface features on sand-sized quartz particles allows description of the genesis of deposits, while the presence of fresh chips on the particle surface suggests a cryogenic impact (Woronko and Pisarska-Jamrozy, 2015; Kurchatova

and Rogov, 2020). The morphology of quartz grains also bears traces of cryogenic impact: the enclosing deposits are characterized by numerous quartz grains with chips and conchoidal fractures of a cryogenic nature (Fig 5); there are grains that combine the initial signs of eolian activity, subsequently subjected to cryogenic crushing (Fig. 5g). However, it should be noted that similar features have been interpreted as indicating glacial grinding during production of the silt particles forming loess (Költringer et al., 2021a), which is consistent with a dominant northern ice-sheet source, as demonstrated using detrital zircon U-Pb analyses on Lower Volga loess (Költringer et al., 2022). In any case, the micromorphological properties identified in thin sections, which were shown for the Srednyaya Akhtuba in the MIS 5 paleosols, present an argument in favor of the cryogenic genesis of the structures (Makeev et al., 2021). Micro-wedges in paleosols of three pedogenetic levels (PL 5, MIS 5a; PL6, MIS 5c; and PL7, MIS 5e), that are filled with silty effervescent material from the overlying loess, are especially clearly visible against the dark humus horizon in the studied pedocomplexes.

Paleogeographic conditions for the development of the cryogenic stages in the LVR

Stage I (95–90 ka)
The final stage of the late Khazar transgression (Hyrcanian stage) is reconstructed during this period in the Caspian Sea region. According to recent interpretations (Yanina, 2020), the transgression developed in a humid epoch with abundant river inflow. The sea level was ~20–30 m higher than now, the waters of the Hyrcanian basin entered along the Volga valley, forming a wide estuary. The beginning of the Valdai glaciation is also noted in the EEP for this time, in the second half of MIS 5 (Velichko, 2002). For this large region, phase II of the Smolensk cryogenic stage is observed here in MIS 5b (Velichko et al., 2017). In the LVR, we reconstruct the existence of a thin continuous permafrost with poor moisture content at that time, which suggests that even during initial late interglacial cooling, the Eurasian permafrost belt extended far south compared with its interglacial limits.

Stage II (75–70 ka)
During the development of this stage, paleogeographic conditions were characterized by the Valdai glaciation on the EEP. In the LVR, this period is also marked by significant changes: the beginning of a deep Atelian regression of the Caspian Sea; and a change in climatic parameters from humid and relatively warm (the end of soil formation MIS 5a) to cold, dry, and windy (the beginning of the formation of loess deposits MIS 4) (Velichko, 1973; Költringer et al., 2021a, 2021b). On the one hand, for this period we demonstrate similar structures in sections located relatively far from each other but within the same type of sediment (e.g., Srednyaya Akhtuba and Bataevka)—narrow and vertically long structures in paleosol filled with loess material. On the other hand, there are clearly different structures in sections at the same latitude but in different genetic types of sediments—narrow and vertically long structures in paleosols filled with loess material in Srednyaya Akhtuba and bag-like structures in alluvium in Raygorod section. This supports the observation that sediment type influences the final shape of structures more than the location of the site (within one region). We reconstruct the existence of a continuous permafrost for this time. Significant areas of the river valley were under the influence of cryogenesis and eolian deflation that supported loess formation at that time.

Stage III (52–45 ka)

During this cryogenic stage (MIS 3c to the first half of MIS 3b), there appears to be some increase in the level of the Caspian Sea, contributing to the penetration of water into the Volga River valley and the thawing of frozen sediments. The Bryansk interstadial, a warm period within the Valdai glaciation, begins in the EEP at that time. Because these structures are recorded in watershed conditions at Raygorod in sediments forming with low moisture content, we conclude that the climate conditions had to be rather cold for cryogenesis to affect the structure of the sediments. Because cryogenic structures of this stage were only found in one section in the LVR, we reconstruct the existence of a thin sporadic permafrost during the MIS 3c that developed in a cold climate but under extremely dry conditions that limited development of cryogenesis.

Stage IV (37–35 ka):

For the MIS 3 period characterized by short warming and moistening phases and a rise in the level of the Caspian Sea, an increase in moisture content in the sediments is typical (recoded in paleosol development in loess: layers 8–6 in Raygorod and 11–6 in Srednyaya Akhtuba). The Volga River channel repeatedly changed its position at that time due to the formation of a large estuary in the valley. The final stage of the Bryansk paleosol formation is identified at that time in the EEP. In the LVR, there was either thin continuous or rare sporadic permafrost, as cryogenesis is only recorded in two sections and represented by weakly developed structures.

Overall, the timing of these permafrost stages suggests more extensive early last glacial permafrost than is widely assumed and demonstrates the sensitivity of the LVR to climatic oscillations. The continental climate combined with a relatively southerly latitude for the region means that the region is a highly sensitive indicator of changes in last glacial permafrost extent and can be used to consider wider forcing of these changes. In this regard, it is striking how the phases of permafrost development follow a broadly 20 ka cycle, with repeated permafrost phases broadly coinciding with precession-driven minima in Northern Hemisphere summer insolation (Berger and Loutre, 1991). Given that the phases of cryogenesis appear to occur in many cases on top of weak soils (Makeev et al., 2021) preserved in the sections, it is plausible that these phases of cryogenesis and permafrost expansion alternated with warmer climate phases, likely with warmer summers and with (perhaps) higher precipitation (Költringer et al., 2021b). As such, while overall ice-sheet expansion was closely linked to eccentricity, repeated extensions and contractions of permafrost were superimposed on this, and likely controlled by precessional cycles and their influence over summer temperatures and seasonality. The LVR is the ideal place to see such changes, as it lies at the limit of the last glacial permafrost belt and is therefore highly sensitive to recording past permafrost extent.

Conclusions

Analysis of multiple subaerial to shallow-marine facies in sediments of the LVR reveals a number of aspects concerning last glacial permafrost.

The morphology of the structures, distribution of the CWI, morphoscopy of quartz grains, and microstructure of the deposits confirm the cryogenic origin of many geologic forms identified in the late Pleistocene deposits for a number of cryogenic horizons in the LVR.

We present for the first time unambiguous evidence of development of cryogenesis in the northern Caspian Lowland recorded in various structures and layers. Cryogenesis affected the main types of sediments (loess, paleosols, and alluvium) and formed sporadic or continuous permafrost depending on the climate conditions. Several layers of cryogenic structures show that during the Late Quaternary, permafrost expanded to the southeast of the EEP repeatedly and to a much more southerly extent than previously reconstructed.

The results of luminescence dating and the correlation of cryogenic horizons within studied sections made it possible to identify four stages in the development of cryogenesis in the LVR in the late Pleistocene.

The conditions during loess accumulation were severe and cold; cryogenesis was reflected in more clayey and more humid deposits, that is, in paleosols. The most severe conditions in the LVR with permafrost and negative soil temperatures existed at the boundary between MIS 5a/MIS 4 (cryogenic stage II, 75–70 ka) and were reflected in all the studied sections in the form of regionally widespread thin pseudomorphs in Srednyaya Akhtuba, Leninsk, and Bataevka, as well as in bag-like structures in alluvium in Raygorod.

Because the climate parameters in the studied region are quite homogeneous, the reconstruction took into account local climatic features, composition of sediments, humidity, and the history of the region. The formation of wedge-shaped cryogenic structures can be explained by freezing of moisture-saturated sediments, which is confirmed by measuring the CWI in the horizons affected by cryogenesis, indicating the development of a thin permafrost.

The repeated expansion and contraction of permafrost in the late Pleistocene revealed in our study demonstrates that (1) the permafrost zone of the last glaciation in this part of Eurasia was highly dynamic; (2) sufficiently cold conditions for continuous permafrost development in this area were established already at the end of MIS 5; and (3) precession-driven changes in summer insolation in the Northern Hemisphere were probably major controls over permafrost expansion and contraction.

References

Berger, A., Loutre, M.F., 1991. Insolation values for the climate of the last 10 million years, *Quaternary Science Reviews* **10**, 297–317.

Buylaert, J.P., Jain, M., Murray, A.S., Thomsen, K.J., Thiel, C., Sohbati, R., 2012. A robust feldspar luminescence dating method for Middle and Late Pleistocene sediments. *Boreas* **41**, 435–451.

Deng, J., Wang, L., Zhang, Z.Z., Bing, H., 2010. Microstructure characteristics and forming environment of late Quaternary Period loess in the Loess Plateau of China. *Environmental Earth Sciences* **59**, 1807–1817.

Fedorov, P.V., 1957. *Stratigrafiya chetvertichnykh otlozheniy i istoriya razvitiya Kaspiyskogo morya* [Stratigraphy of Quaternary deposits and the history of

the development of the Caspian Sea]. Trudy GIN AN SSSR, Vol. 10. AN SSSR, Moscow.

Feng, L., Zhang, M., Jin, Zh., Zhang, Sh., Sun, P., Gu, T., Liu, X., *et al.*, 2021. The genesis, development, and evolution of original vertical joints in loess. *Earth-Science Reviews* **214**, 103526.

Gelfan, A., Kalugin, A., 2021. Permafrost in the Caspian basin as a possible trigger of the late Khvalynian Transgression: testing hypothesis using a hydrological model. *Water Resources* **48**, 831–843.

Kalinska-Nartiša, E., Lamsters, K., Karušs, J., Krievans, M., Rečs, A., Meija, R., 2017. Quartz grain features in modern glacial and proglacial environments: a microscopic study from the Russell Glacier, southwest Greenland. *Polish Polar Research* **38**, 265–289.

Költringer, C., Bradák, B., Stevens, T., Almqvist, B., Banak, A., Linder, M., Kurbanov, R., *et al.*, 2021a. Palaeoenvironmental implications from Lower Volga loess—joint magnetic fabric and multi-proxy analyses. *Quaternary Science Reviews* **267**, 107057.

Költringer, C., Stevens, T., Bradák, B., Almqvist, B., Kurbanov, R., Snowball, I., Yarovaya, S., 2021b. Enviromagnetic study of Late Quaternary environmental evolution in Lower Volga loess sequences, Russia. *Quaternary Research* **103**, 49–73.

Költringer, C., Stevens, T., Linder, M., Baykal, Y., Ghafarpour, A., Khormali, F., Taratunina, N., Kurbanov, R., 2022. Quaternary sediment sources and loess transport pathways in the Black Sea–Caspian Sea region identified by detrital zircon U-Pb geochronology. *Global and Planetary Change* **209**, 103736.

Konishchev, V.N., 1981. *Formirovaniye sostava dispersnykh porod v kriolitosfere* [Formation of the composition of dispersed rocks in the cryolithosphere]. Nauka, Novosibirsk.

Konishchev, V.N., 1999. Evolyutsiya temperatury porod arkticheskoy zony Rossii v verkhnem kaynozoye [Temperature evolution of rocks in the Arctic zone of Russia in the Upper Cenozoic]. *Earth's Cryosphere* **3**(4), 39–47.

Konishchev, V.N., Lebedeva-Verba, M.P., Rogov, V.V., Stalina, E.E., 2005. *Kriogenez sovremennykh i pozdnepleystotsenovykh otlozheniy Altaya i periglyatsial'nykh oblastey Yevropy* [Cryogenesis of modern and late Pleistocene deposits of Altai and periglacial regions of Europe]. GEOS, Moscow.

Konishchev, V.N., Rogov, V.V., 1994. *Metody kriolitologicheskikh issledovaniy* [Methods of cryolithological research]. MSU, Moscow.

Koriche, S.A., Singarayer, J.S., Cloke, H.L., Valdes, P.J., Wesselingh, F.P., Kroonenberg, S.B., Wickert, A.D., Yanina, T.A., 2022. What are the drivers of Caspian Sea level variation during the late Quaternary? *Quaternary Science Reviews* **283**, 107457.

Krinsley, D.H., Doornkamp, J.C., 1973. *Atlas of Quartz Sand Surface Textures*. Cambridge University Press, Cambridge.

Kurbanov, R., Murray, A., Thompson, W., Svistunov, M., Taratunina, N., Yanina, T., 2021. First reliable chronology for the early Khvalynian Caspian Sea transgression in the Lower Volga River valley. *Boreas* **50**, 134–146.

Kurbanov, R.N., Belyaev, V.R., Svistunov, M.I., Butuzova, E.A., Solodovnikov, D.A., Taratunina, N.A., Yanina, T.A., 2023. New data on the age of the early Khvalynian transgression of the Caspian Sea. [In Russian.] *Izvestiya Rossiyskoy Akademii Nauk, Seriya Geograficheskay V* **87**, 403–419.

Kurbanov, R.N., Buylaert, J.-P., Stevens, T., Taratunina, N.A., Belyaev, V.R., Makeev, A. O., Lebedeva, M.P., *et al.*, 2022. A detailed luminescence chronology of the Lower Volga loess-palaeosol sequence at Leninsk. *Quaternary Geochronology* **73**, 101376.

Kurchatova, A.N., Rogov, V.V., 2020. *Electron Microscopy in Geocryology*. TIU, Tyumen, Russia.

Lebedeva, M., Makeev, A., Rusakov, A., Romanis, T., Yanina, T., Kurbanov, R., Kust, P., Varlamov, E., 2018. Landscape dynamics in the Caspian Lowlands since the last deglaciation reconstructed from the pedosedimentary sequence of Srednaya Akhtuba, southern Russia. *Geosciences* **8**, 492.

Makeev, A., Lebedeva, M., Kaganova, A., Rusakov, A., Kust, P., Romanis, T., Yanina, T., Kurbanov, R., 2021. Pedosedimentary environments in the Caspian Lowland during MIS 5 (Srednaya Akhtuba reference section, Russia). *Quaternary International* **590**, 164–180.

Moskvitin, A.I., 1962. *Pleystotsen Nizhnego Povolzh'ya* [Pleistocene of the Lower Volga region]. Trudy GIN AN SSSR, Vol. 64. AN SSSR, Moscow.

Murray, A.S., Marten, R., Johnston, A., Martin, P., 1987. Analysis for naturally occurring radionuclides at environmental concentrations by gamma spectrometry. *Journal of Radioanalytical and Nuclear Chemistry* **115**, 263–288.

Murray, A.S., Thomsen, K.J., Masuda, N., Buylaert, J.-P., Jain, M., 2012. Identifying well-bleached quartz using the different bleaching rates of quartz and feldspar luminescence signals. *Radiation Measurements* **47**, 688–695.

Panin, A.V., Sidorchuk, A.Yu, Ukraintsev, V.Yu., 2021. The contribution of glacial melt water to annual runoff of River Volga in the last glacial epoch. *Water Resources* **48**, 877–885.

Popov, A.I., 1960. Periglyatsial'nyye obrazovaniya Severnoy Yevrazii i ikh geneticheskiye tipy [Periglacial formations of Northern Eurasia and their genetic types]. In: *Periglyatsial'nyye yavleniya na territorii SSSR* [Periglacial phenomena on the territory of the USSR]. MGU, Moscow, pp. 10–36.

Popov, A.I., 1967. Loess and loess-like rocks as a product of cryolithogenesis. [In Russian.] *Vestnik MSU, seria geograficheskaya* **6**, 43–48.

Railsback, L.B., Gibbard, P.L., Head, M.J., Voarintsoa, N.R.G., Toucanne, S., 2015. An optimized scheme of lettered marine isotope substages for the last 1.0 million years, and the climatostratigraphic nature of isotope stages and substages. *Quaternary Science Reviews* **111**, 94–106.

Rasmussen, C.F., Christiansen, H.H., Buylaert, J.-P., Cunningham, A., Schneider, R., Knudsen, M., Stevens, T., 2023. High-resolution OSL dating of loess in Adventdalen, Svalbard: Late Holocene dust activity and permafrost development. *Quaternary Science Reviews* **310**, 108137.

Shkatova, V.K., 1975. Stratigrafiya pleystotsenovykh otlozheniy nizov'yev rek Volgi i Urala i ikh korrelyatsiya [Stratigraphy of Pleistocene deposits in the lower reaches of the Volga and Ural rivers and their correlation]. PhD thesis. VSEGEI, Leningrad.

Streletskaya, I.D., 2017. Wedge-shaped structures on the southern coast of the Gulf of Finland. [In Russian.] *Earth's Cryosphere* **21**(1), 3–12.

Svitoch, A.A., 2014. *The Great Caspian: Structure and History of Development*. [In Russian.] MSU, Moscow.

Svitoch, A.A., Yanina, T.A., 1997. *Chetvertichnyye otlozheniya poberezhiy Kaspiyskogo* morya [Quaternary deposits of the coasts of the Caspian Sea]. RASKHN, Moscow.

Sycheva, S.A., 2012. Paleofrost events in the periglacial region of the Russian Plain at the end of the Middle and Late Pleistocene. [In Russian.] *Earth's Cryosphere* **16**(4), 45–56.

Taratunina, N.A., Buylaert, J.-P., Kurbanov, R.N., Yanina, T.A., Makeev, A.O., Lebedeva, M.P., Utkina, A.O., Murray, A.S., 2022. Late Quaternary evolution of lower reaches of the Volga River (Raygorod section) based on luminescence dating. *Quaternary Geochronology* **72**, 101369.

Taratunina, N., Rogov, V., Streletskaya, I., Thompson, W., Kurchatova, A., Yanina, T., Kurbanov, R., 2021. Late Pleistocene cryogenesis features of a loess-paleosol sequence in the Srednyaya Akhtuba reference section, Lower Volga River valley, Russia. *Quaternary International* **590**, 56–72.

Vasiliev, Yu.M., 1961. *Antropogen Yuzhnogo Zavolzh'ya* [Anthropocene of the southern Trans-Volga region]. AN SSSR, Moscow.

Velichko, A.A., 1973. *Prirodnyy protsess v pleystotsene* [Natural process in the Pleistocene]. Nauka, Moscow.

Velichko, A.A. (Ed.), 2002. *Dinamika landshaftnykh komponentov i vnutrennikh morskikh basseynov Severnoy Yevrazii za posledniye 130 000 let* [Dynamics of landscape components and inland marine basins of northern Eurasia over the past 130,000 years]. GEOS, Moscow.

Velichko, A.A., Borisova, O.K., Kononov, YU.M., Konstantinov, Ye.A., Kurbanov, R.N., Morozova, T.D., Panin, P.G., *et al.*, 2017. Rekonstruktsiya sobytiy pozdnego pleystotsena v periglyatsial'noy zone yuga Vostochno-Yevropeyskoy ravniny [Reconstruction of Late Pleistocene events in the periglacial zone of the south of the East European Plain]. *Doklady Akademii* **475**, 448–452.

Velichko, A.A., Morozova, T.D., Nechayev, V.P., Porozhnyakova, O.M., 1996. *Paleokriogenez, pochvennyy pokrov i zemledeliye* [Paleocryogenesis, soil cover and agriculture]. Nauka, Moscow.

Vos, K., Vandenberghe, N., Elsen, J., 2014. Surface textural analysis of quartz grains by scanning electron microscopy (SEM): from sample preparation to environmental interpretation. *Earth-Science Reviews* **128**, 93–104.

[VSEGEI] Russian Geological Research Institute, 2014. Mezhregionalnaya stratigraficheskaya skhema kvartera territorii Rossiyskoy Federatsii [Interregional stratigraphic scheme of the quarter of the territory of the Russian Federation]. Supplement to the Map of Quaternary Formations of the Territory of the Russian Federation. 1:2,500,000. St. Petersburg.

Woronko, B., Pisarska-Jamrozy, M., 2015. Micro-scale frost weathering of sand-sized quartz grains. *Permafrost and Periglacial Processes* **27**, 109–122.

Yanina, T., 2020. Environmental variability of the Ponto-Caspian and Mediterranean Basins during the last climatic macrocycle. *Geography, Environment, Sustainability* **13**, 6–23.

Yanina, T.A., Svitoch, A.A., Kurbanov, R.N., Myurrey, E.S., Tkach, N.T., Sychev, N.V., 2017. Experience in dating Pleistocene deposits of the Lower Volga region by optically stimulated. [In Russian.] *Vestnik MSU, seria geograficheskaya* **1**, 21–29.

Zhai, J., Zhang, Z., Melnikov, A., Zhang, M., Yang, L., Jin, D., 2021. Experimental study on the effect of freeze-thaw cycles on the mineral particle fragmentation and aggregation with different soil types. *Minerals* **11**, 913.